PCCP

Accepted Manuscript

ROYAL SOCIETY OF CHEMISTRY

www.rsc.org/pccp

Journal Name

RSCPublishing

ARTICLE

A DFT Study of the carboxymethyl-phosphatidylethanolamine formation from glyoxal and phosphatidylethanolamine surface. Comparison with the formation of N(ϵ)-(carboxymethyl)lysine from glyoxal and L-lysine.

Cite this: DOI: 10.1039/xoxxoooooox

Received ooth January 2012,
Accepted ooth January 2012

DOI: 10.1039/xoxxoooooox

www.rsc.org/

C. Solís-Calero[a], J. Ortega-Castro[a,]*, A. Hernández-Laguna[b], J. Frau[a], F. Muñoz[a]

Mechanisms for generation of carboxymethyl compounds Nε-(carboxymethyl)lysine (CML) and carboxymethyl-phosphatidylethanolamine (CM-PE), from the reactions between glyoxal and L-lysine and glyoxal and phosphatidylethanolamine (PE) by DFT method at PBE/DNP level of theory were carried out. In order to study the reaction with PE, a periodic model of the PE-surface was built, the starting surface model includes two molecules of PE, a molecule of mono hydrated form of glyoxal, and five water molecules as explicit solvent that form a hydrogen bond network, which are involved in the reactions by stabilizing reaction intermediates and transition states and as proton-transfer carriers, important in all steps of reactions. Both reactions take place in three steps, namely: 1) Carbino-diol-amine formation; 2) dehydration; 3) rearrangement into carboxymethyl final products. The rate-limiting step for the formation of CML/CM-PE was the dehydration stage. The comparison of both reactions in their equivalent stages, showed a catalytic role of the PE surface, it is highlighted in the case of dehydration step where its relative free energy barrier had a value of 5.3 kcal mol^{-1} lower than the obtained in L-lysine/glyoxal system. This study gives insights about the active role of phospholipid surfaces on some chemical reactions that occur above it. Our results also give support to consider the pathway of formation of CML and CM-PE from reactions between glyoxal and L-lysine and glyoxal and PE, as an alternative pathway for generation of these advanced glycation end-products (AGEs).

Introduction

Advanced glycation end-products are a heterogeneous group of bioactive molecules that are involved in the development of diabetes, atherosclerosis, chronic kidney diseases, and other diseases. Endogenous advanced glycation end-products (AGEs) are generated by the non-enzymatic glycation of proteins, lipids, and nucleic acids through their free amine groups, especially under hyperglycemic conditions in diabetes[1,2]. One of the major AGEs of proteins widely found in vivo is the Nε-(carboxymethyl)lysine (CML), which can be formed by three concurrent mechanisms[3], having been studied extensively its processing and relationship with some diseases[1,4,5]. In the classical protein glycoxidation pathway the Schiff base, which results from the reaction between the lysine amino acid and glucose, rearranges into the Amadori product, which is then oxidatively fragmented to give CML, among other products[6,7]. In the 'autoxidative glycosylation' pathway, CML is formed by the reaction between lysine and glyoxal, the latter of which results from metal-catalysed autoxidation of glucose[8-10]. In a third mechanism, known as Namiki pathway, the fragmentation and the oxidation of the Schiff base give as products two carbon fragments including free glyoxal, which can subsequently forms CML[11,12].

The non-enzymatic modification of amino groups in aminophospholipids also produce carboxymethyl compounds, as carboxymethyl-phosphatidylethanolamine (CM-PE), whose generation in human erythrocytes and blood plasma has been

demonstrated experimentally[13-15]. It is possible to hypothesise that the generation of CM-PE could proceed by similar mechanisms than CML[13,16,17]. As its Amadori-PE precursor, AGE-PE could trigger pathological processes[18,19], being suggested useful as a potentially sensitive marker for reflecting hyperglycemic conditions in the early stage of diabetes[13,20].

Glyoxal is a reactive carbonyl, which can be generated endogenously from the glucose autoxidation[9,21,22] as well as in the process of the oxidative degradation of polyunsaturated fatty acids[23] and myeloperoxidase-mediated degradation of serine at sites of inflammation[24]. It is one of the α-oxoaldehydes which act as a key factor in the carbonyl stress resulting from impaired balance between the generation of carbonyl intermediates and efficiency of scavenger pathway[22,25]. Glyoxal is also a potent glycating agent leading to the formation of advanced glycation endproducts (AGEs)[26,27]. This reaction also progresses on amino residues of membrane lipids such as phosphatidylethanolamine (PE), being one of the pathways that yields CM-PE[13,28].

AGEs formation on cell membrane components such as PE has medical relevance since these lipids are vital for the maintenance of cellular integrity and survival. Their modification could result in the membrane structure deterioration and dysfunction into the cell. While AGEs generation from non-enzymatic protein glycation and its involvement in several diseases have been thoroughly investigated[2,29,30], less attention has been paid to AGEs generation from reactions of phospholipids with free amino groups such as PE and phosphatidylserine[13,28,31-33].

Inhibition of AGEs formation is a potential strategy for the prevention of clinical diabetes complications and other diseases, being the description of the reactions involved in AGEs formation relevant for obtaining this purpose. However, there is a lack of theoretical studies describing the mechanisms of these reactions at the atomic level. There is only a theoretical study on a mathematical model that describes the generation of CML[3]. Our group has previous experimental and theoretical studies about Schiff base formation and Amadori rearrangement mechanisms in different molecular systems[34-43]. However, this is the first time we modelled the reaction mechanisms for obtaining AGEs as CML and CM-PE.

The first comprehensive model of the biological membranes, the 'fluid mosaic model', assumes the lipid bilayer to be a passive structure fulfilling two basic functions: supporting proteins and forming a barrier for dissolved molecules in the aqueous phase[44]. However, experimental data obtained in studies on biological and model membrane systems made lipid bilayer be also recognized as a potent enhancer and regulator of surface associated reactions[45-47]. It could also enhance the ability of protons to diffuse promptly along the membrane through a hydrogen bonded network of water molecules and charged or/and polar groups of phospholipids at the surface[48]. The phospholipid exhibited reactive properties, as it has been shown by several experimental studies[35,36,49-53]. Our group developed a periodic model of PE-surface in order to study theoretically the reactivity above phospholipids surface. In this model, we have studied the decomposition of H_2O_2, the formation of Schiff bases and the Amadori rearrangement[34,37,54]. The obtained results showed the catalytic potential of phospholipid surfaces for participating in other reactions that occur on the cell membrane surface.

Therefore, the aim of this study is to obtain and describe, at DFT level of theory, the mechanisms for formation of CML and CM-PE from reactions between glyoxal and L-lysine and phosphatidylethanolamine (PE), respectively. We also analyze comparatively the influence of the chemical environment on the reaction, modelling the reaction for formation of CML in an aqueous environment, and the reaction for formation of CM-PE, above a PE-surface, using periodic boundary conditions. This work also shows the role of water solvent molecules, acting catalytically via an H-atom-transfer mechanism during the reaction.

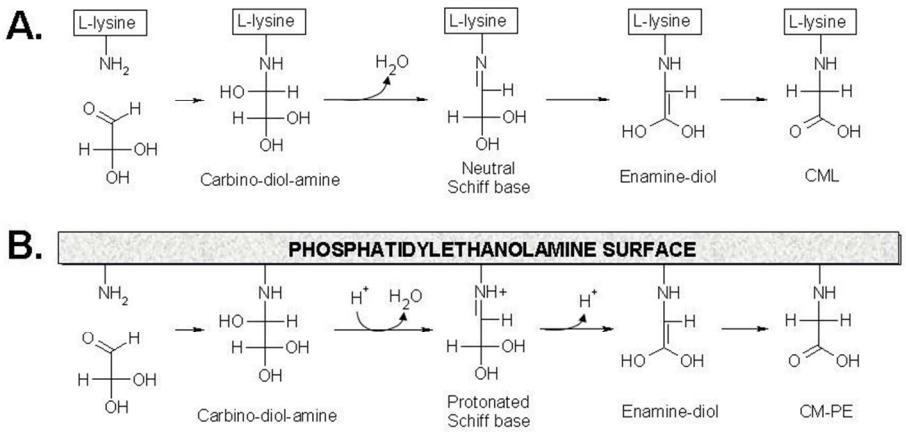

Scheme 1 Reactions pathways for the generation of carboxymethyl compounds CML (A) and CM-PE (B).

Methodology

To study the generation of carboxymethyl compounds, CML and CM-PE, we used two models including L-lysine and PE respectively, as free amino-containing reagents for their reaction with glyoxal (scheme 1). The differences in adjacent groups could let us evaluate the possible influence of these groups in the reactions. In the case of PE, it is possible to evaluate additionally the influence of an environment different to aqueous solvent.

The PE surface model was designed from the crystal structure of 1,2-Dilauroyl-DL-phosphatidylethanolamine[55]. The PE surface model was represented using a three-dimensionally periodic slab model. The supercell (Fig. 1) contained two molecules of truncated PE, a glyoxal monohydrate molecule, and five water molecules as explicit solvent in a hydrogen-bond network along the polar heads of phospholipids. The periodic boundary conditions made possible to obtain a surface model of a layer of phospholipids, useful for studying theoretically the reaction on an environment different to aqueous solvent. The mechanism of reaction between L-lysine and glyoxal was done without periodic boundary conditions, but also including nineteen water molecules as explicit solvent and glyoxal monohydrate molecule. In all cases, an additional solvent environment was modelled via the conductor- like screening model (COSMO)[56-58]. The purpose of including water molecules in both molecular models was not exclusively to simulate a water solvation environment; rather, the water molecules were intended to act as reactive species facilitating several steps of the studied reactions.

All the calculations were performed in the framework of DFT with package DMol3 of Accelrys, Inc.[59-61], using double numerical with polarization (DNP) basis set[61] and Perdew–Burke–Ernzerhof (PBE) generalized gradient approximation (GGA) exchange-correlation functional[62,63]. The DNP numerical basis set is comparable to Gaussian 6-31G(d,p)[64], minimizes the basis set superposition error[65], and its accuracy for describing hydrogen-bond strengths showed a good agreement with experimental values[66]. The maximum number of numerical integration mesh points available in DMol3 was chosen for our computations, the threshold of density matrix convergence was set to 10^{-6}. A Fermi smearing of 0.005 Hartree and a real-space cutoff of 4.5 Å were also used to improve the computational performance.

The reactants and stationary points generated during carboxymethyl compounds formation were modelled in Materials Visualizer, and optimized using the conjugated gradient algorithm. The transition state (TS) searches were performed with the complete LST/QST method[67]. In this method, the linear synchronous transit (LST) maximization was performed, followed by an energy minimization in directions conjugating to the reaction pathway to obtain an approximated TS. The approximated TS was used to perform quadratic synchronous transit (QST) maximization and then another conjugated gradient minimization was performed. The cycle was repeated until a stationary point was located. The obtained TS was optimized via eigenvector following, searching for an energy maximum along one previous selected normal mode and a minimum along all other nodes, using the Newton-Raphson method. After this procedure, one transition state was found for each reaction step. Each TS structure was characterized by a vibrational analysis with exactly one imaginary frequency.

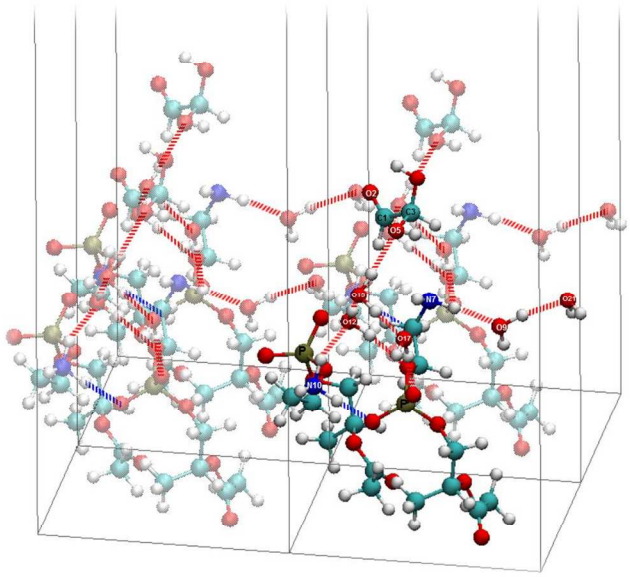

Fig. 1 Periodic model of phosphatydilethanolamine surface. Section of the initial model for two phosphatidylethanolamine molecules, monohydrated form of glyoxal and the water hydrogen-bond network. The atoms belonging to one representative cell are represented by balls and sticks. Atoms in neighboring cells are shaded. Phosphorus and reactive atoms are labelled, and dotted lines represent hydrogen bonds.

Results and discussion

Schemes 2 and 3 showed the overall processes for reactions of formation of CML and CM-PE, respectively. Both mechanisms involved three steps: (1) carbino-diol-amine formation (structures 1-5 for CML, and 1-7 for CM-PE) (2) dehydration (structures 5-7 for CML, and 7-9 for CM-PE) (3) rearrangement and carboxymethyl product generation (structures 7-11 for CML, and 9-13 for CM- PE). The second step is the rate-determining step of the process, what is consistent with available experimental evidence for reactions with similar mechanisms[13]. The free energy (ΔG) values for each structure in both reactions are listed in table 1, and the ΔG profiles are shown in Fig. 2. Tables 2 and 3 show structurally data (distances, bond angles) for each intermediate and the transition states of studied reactions.

In all the studied systems the water molecules form a hydrogen bond network with hydrogen bond donors or acceptors groups of reagents and intermediates of reactions. These networks play a prominent role in all proton transfers.

Additionally, included water molecules can influence the free energy barriers in the reaction steps, by electrostatic stabilization of the ionic transition states and intermediates structures, and acting as a proton-transfer carrier.

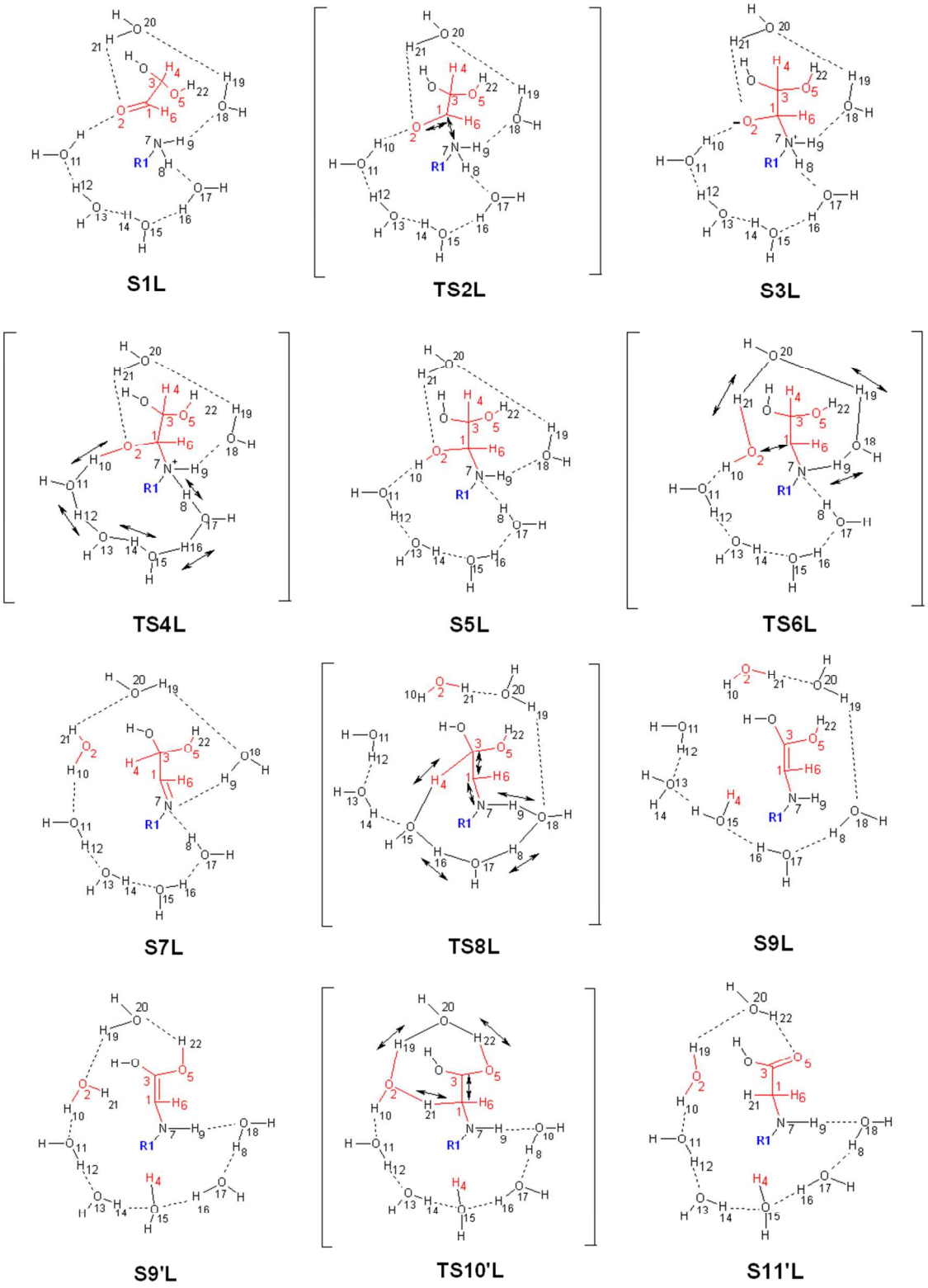

Scheme 2. Mechanism of formation of N(ε)-carboxymethyl-Lysine from glyoxal and L-lysine. Dotted lines represent hydrogen bonds and arrows represent changes in the electronic density and proton transfers.

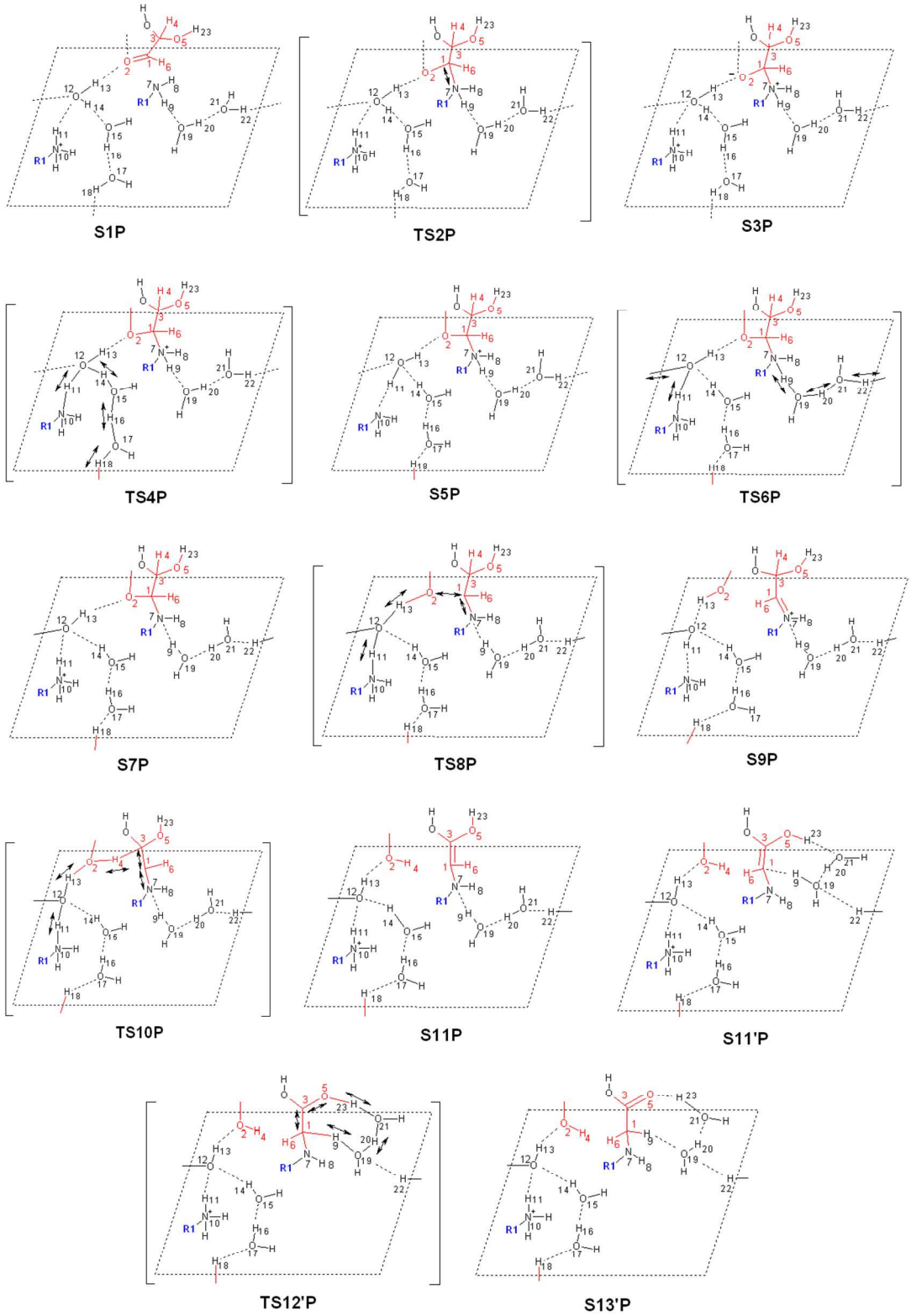

Scheme 3. Mechanism of carboxymethyl-PE formation from glyoxal and PE, using periodic boundary conditions. Dotted lines represent hydrogen bonds and arrows represent changes in the electronic density and proton transfers.

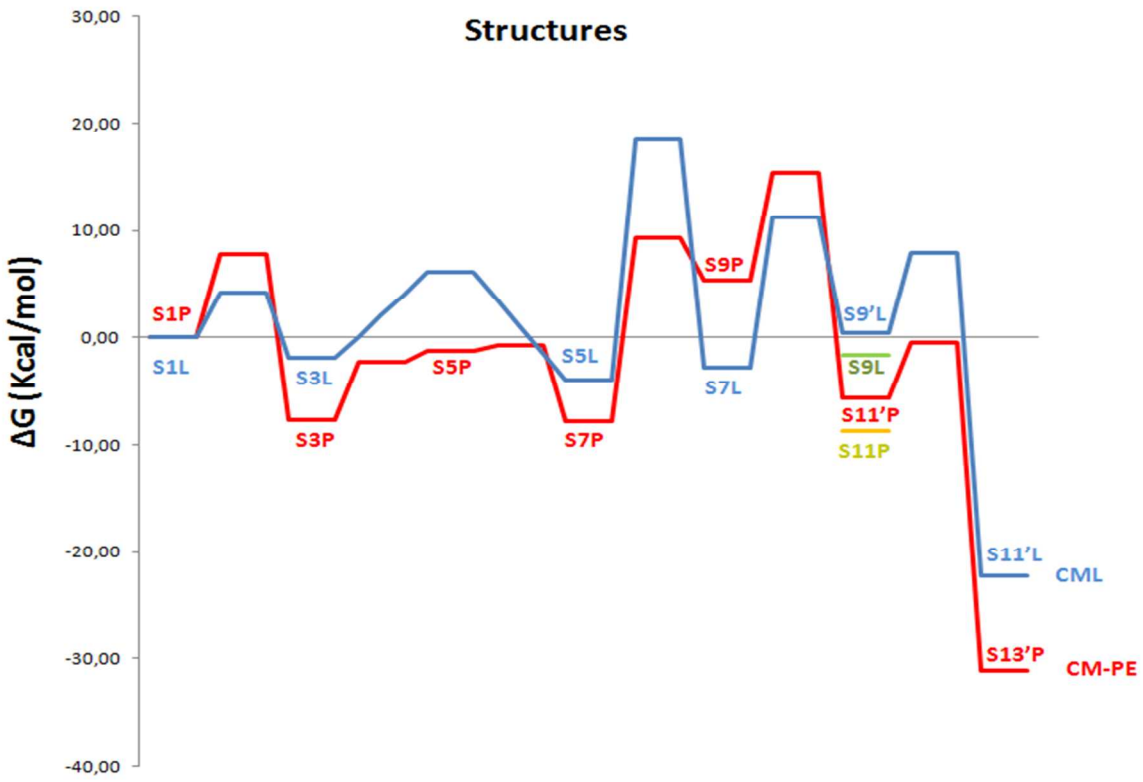

Figure 2. Free energy profiles for CML formation mechanism (blue line) and CM-PE formation mechanism (red line). Free energy values comparison of S9L (green line) and S9'L (blue line) structures and S11P (yellow line) and S11'P (red line) structures.

Table 1. Relative free energies of the structures of the studied reaction paths.

L-lysine		Phosphatydilethanolamine	
Structures	**ΔG (kcal mol^{-1})**	**Structures**	**ΔG (kcal mol^{-1})**
S1L	0.00	S1P	0.00
TS2L	4.12	TS2P	7.79
S3L	-1.90	S3P	-7.68
		TS4P	-2.26
TS4L	6.05	S5P	-1.27
		TS6P	-0.68
S5L	-3.93	S7P	-7.83
TS6L	18.49	TS8P	9.29
S7L	-2.80	S9P	5.34
TS8L	11.31	TS10P	15.41
S9L/S9'L	-1.64/ 0.38	S11P/S11'P	-8.75/ -5.67
TS10'L	7.85	TS12'P	-0.42
S11'L	-22.22	S13'P	-31.05

The conversion of glyoxal from its conventional non hydrated form to its monohydrate form was studied (scheme 4). We have considered glyoxal monohydrate molecule as part of the initial structures of both molecular systems (S1L and S1P in schemes 2 and 3). In solution at low concentrations, glyoxal is present primarily as hydrated monomer with one or both aldehydic groups forming a geminal diol[68]. Due to its high reactivity, at high concentrations it also could be in the form of hydrated oligomers[69]. According to the evaluated mechanisms, the first hydration of glyoxal occurs by nucleophilic addition of a water molecule to one of the glyoxal carbonyl groups and a concerted proton transfer from the oxygen atom of the added water molecule to the oxygen of the carbonyl group, having as a bridge two water molecules (scheme 4). The obtained free energy barrier for this reaction was 5.81 kcal mol^{-1}, having the monohydrated form of glyoxal a free energy value 6.88 kcal mol^{-1} lower than the non hydrated form, and close to the values obtained for hydrations of other carbonyl compounds such as methylglyoxal[70].

a) Carbino-diol-amine formation. The starting points for these stepwise processes are the structures S1L and S1P (Schemes 2 and 3, respectively). The relative energy barriers of the direct additions of the amino group (N7) to the carbonyl group at the monohydrated form of glyoxal (C1) had values of 4.12 and 7.79 kcal mol^{-1} for L-lysine and PE surface, respectively. These values are low in comparison to those obtained by other studies with different levels of calculation. In the reaction between dimethylamine and propanal, the values

for the free energy of activation were 34.90 and 38.40 kcal mol^{-1} after gas-phase calculations at MP2/6-31G*//6-31G* and mPW1PW91/6-311+G**//6-31G*, respectively[71]. The relative energy barrier for this addition in the reaction between proline and acetone had a value of 37.79 kcal mol^{-1} after gas-phase B3LYP/6-311G(d,p) calculations[72]. This step had a relative energy barrier value of 9.7 kcal mol^{-1} in the reaction of Schiff Base formation between a pyridoxamine analog and acetaldehyde with B3LYP/6-31+G(d,p) level of calculation[73]. In this late study, when CPCM implicit solvent model was included the barrier was only modified to 9.4 kcal mol^{-1}. The lower values in the cases of L-lysine and PE with glyoxal, can be ascribed to the presence of an explicit solvent in the models, that allows to form hydrogen bonds with the reactants and products alike, thereby facilitating the addition of the amino group to the carbonyl carbon.

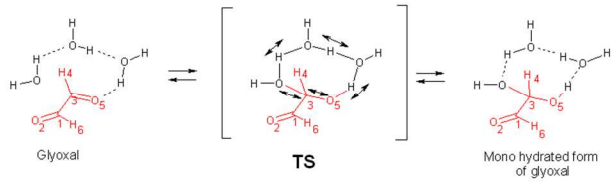

Scheme 4. Mechanism for the first hydration of glyoxal. Glyoxal atoms keep their labels according the L-lysine/glyoxal system. Dotted lines represent hydrogen bonds and arrows represent changes in the electronic density and proton transfers.

The zwitterionic form of the carbino-diol-amine from PE (S3P in scheme 3) had a relative free energy 5.78 kcal mol^{-1} lower than formed by reaction with L-lysine (S3L in scheme 2) (Fig. 2). The charged and polar groups in PE-surface could stabilize the hydrogen bond network. The presence of polar and charged groups in the PE surface imposes limitations on the mobility of the water molecules on its surface, polarizing them and also the reactive molecules. Theoretical studies show that the water molecules near a polar surface are oriented by an electrostatic field associated with lipid residual charges[74,75]. The amount of water, its structure and mobility change is a function of the distance from the aqueous phase[76-78].

In both models, the water molecules are direct participant in the reactions instead of a simple passive dielectric medium, acting as a bridge in the proton transfer between proton donors and acceptors groups. During the conversion of the zwitterionic form of the carbino-diol-amine to its neutral form there are proton transfers, having as bridges water molecules that connect reactive groups. In the case of L-lysine/glyoxal system, a proton transfer is directly done from an amine group (N7 in structure S3L, scheme 2) to the charged oxygen atom (O2 in structure S3L, scheme 2) through two water molecules. In the case of PE surface/glyoxal system, this process is done through two transition states (TS4P and TS6P). Initially, a positive charged form of carbino-diol-amine is formed as a intermediate structure (S5P in scheme 3), through a proton transfer from positive charged amine group of other PE molecule in the surface (N10 in structure S3P, scheme 3) to the negative charged oxygen atom (O2 in structure S3P, scheme 3). It is followed by the conversion of this positive charged intermediate to the neutral form of carbino-diol-amine, due to a proton transfer from the positive charged amine group of the carbino-diol-amine to the neutral amine group of the other PE molecule in the surface (TS6P in scheme 3). Both proton transfers needed a chain of three water molecules. The boundary translation invariance of the modelled periodic system is relevant to this study, allowing the equivalent cleavage of bonds and transfer of protons between unit cell images. It is appreciated in the proton transfer from O17 to O2 (TS4P in scheme 3), and from O21 to O12 (TS6P in scheme 3).

If the free energy barriers for the conversion of zwitterionic form of the carbino-diol-amine into its neutral form are compared (Fig. 2, table 1), we find a value of 7.95 kcal mol^{-1} in the case of L-lysine/glyoxal system (S3L to S5L), and 7.00 kcal mol^{-1} in the case of PE-surface/glyoxal system (S3P to S7P). These results are similar to those we have obtained for the carbinolamine formation from the reaction between acetaldehyde and PE, and the same aldehyde with glycine[79]. This conversion involves a proton transfer, having as acceptor an alkoxide group, considered generally as strong bases. This fact explained also the relative low free energy barriers for this part of the neutral carbino-diol-amine formation step. What is in accordance with the known reversibility of the reaction in other molecular systems[80,81]. This feature is enhanced in the PE-system, where there is an absence of a free energy barrier in the conversion between the protonated form of carbino-diol-amine from PE to its neutral form, not finding significant differences between the free energy values of TS4P, S5P and TS6P structures (table 1, Fig. 2).

The bond lengths of the alkoxide group (O2 in structures S3L and S3P) are other interesting structural aspects of the conversion of zwitterionic form of the carbine-diol-amine into its neutral form. Other theoretical study showed the oxygen in the alkoxide ions repels charge from the adjacent carbon, and onto the groups attached to this carbon, resulting in a coulombic attraction between the alkoxy oxygen and the carbon that leads to a shorter bond respect to its equivalent alcohol group[82]. Something evidenced in our studied systems, where the values of bond lengths for C1-O2 had a value of 1.35 Å in structures S3L and S3P, respect to values of 1.45 Å in structure S5L (L-lysine/glyoxal system, table 2) and 1.43 Å in structure S7P (PE-surface/glyoxal system, table 3).

b) Dehydration. The next step in the reaction is the dehydration of the carbino-diol-amines to Schiff bases, which involves a protonation of the oxygen atom, breaking of two bonds and formation of two new bonds. In the L-lysine/glyoxal system (S5L to S7L through TS6L in scheme 2, Fig. 3A), a proton is removed concertedly from the amine group of carbino-diol-amine (N7-H9) and transferred to hydroxyl group (H10-O2) through two water molecules to form the leaving group (H10-O2-H21). In the process a double bond is formed N7=C1. In the case of PE surface (S7P to S9P trough TS8P in scheme 3, Fig. 3B), an intermolecular proton transfer occurs from the protonated amino group in the second phospholipid

chain to the oxygen O2 in the carbino-diol-amine generated above PE.

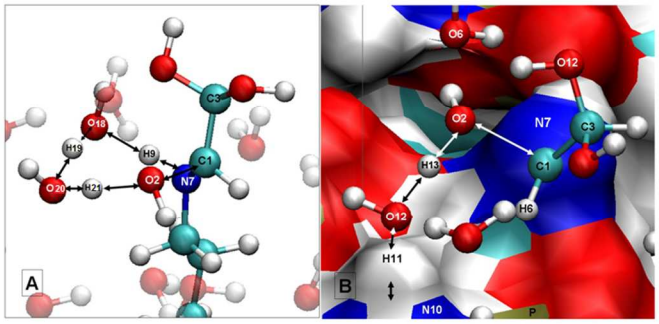

Figure 3. Transition states of dehydration of the carbinolamine molecule. A. From reaction between glyoxal and L-lysine (TS6L). Reactive atoms are labelled, and arrows represent proton transfers. B. From reaction between glyoxal and phosphatidylethanolamine surface (TS8P).

This step is done concertedly with the break of the covalent bond C1-O2 and formation of the π bond N7=C1. In this process we obtain the release of a water molecule (H18-O2-H13) and the generation of a positive charged Schiff base. In the case of Schiff base from L-lysine and glyoxal, the generation of Schiff bases involves the formation of an imine double bond between C1 and N7, being the bond length, reduced from 1.45 (S5L) to 1.27 Å (S7L) (table 2), in the case of Schiff base from PE and glyoxal, this bond length is reduced from 1.45 (S7P) to 1.29 Å (S9P) (table 3).

The relative free energy barriers for this step had values of 22.42 and 17.12 kcal mol^{-1} for L-lysine and PE surface, respectively. These values are slightly high in comparison to those obtained for other reactions. In a DFT study on pyridoxal 5'-phosphate (PLP) transamination of α-amino acids, the total energy barrier for dehydration step had a value of 16.9 kcal mol^{-1} [83]. A DFT study of the Schiff base formation between a pyridoxamine analogue and acetaldehyde or glycolaldehyde provided relative energy barriers from 10 to 15 kcal mol^{-1} [73]. In both cases, other chemical groups in the modelled molecular systems provided additional assistance, explaining their relative lower values. The higher free energy barrier for the L-lysine/glyoxal system in comparison to the PE surface/glyoxal system is attributed to the influence of the PE-surface surroundings, which stabilize the transition state more than in a pure water environment. Charged amine group, of the other PE molecule, acts as a proton donor in the acid-catalyzed dehydration in PE-surface/glyoxal system. It converts a poor leaving group (-O2H18 in scheme 3) into a good leaving group. Then, a water molecule, stabilized by a hydrogen bond network above PE-surface, acts efficiently as a bridge in the proton transfer from the charged amine group to the hydroxyl group. This is difficult to replicate in the L-lysine/glyoxal system, where the proton transfer is done through two water molecules (TS6L, scheme 2), explaining its higher free energy barrier (Fig. 2, table 1).

The neutral Schiff base generated from L-lysine and glyoxal is more stable than the positive charged Schiff base, from PE and glyoxal (Fig. 2, table 1). The decreased electrophilicity of the imine double bond in comparison to an equivalent carbonyl bound is accounted for by the lower electronegativity of nitrogen compared to that of oxygen. Therefore, the double bond is less polarised, and in consequence the partial charge at the imine carbon atom is less positive, and the dipole moment is weaker than the corresponding in the carbonyl group. When the nitrogen of the double bond is protonated, it is generated an iminium salt, increasing its electrophilicity, and as a consequence, its reactivity is also increased and its stability reduced. This general characteristic of conjugated imines and iminium salts is taken into account when imino compounds are used for synthesis of nitrogen-containing compounds, being done the activation of their imino carbons through their iminium salts[84].

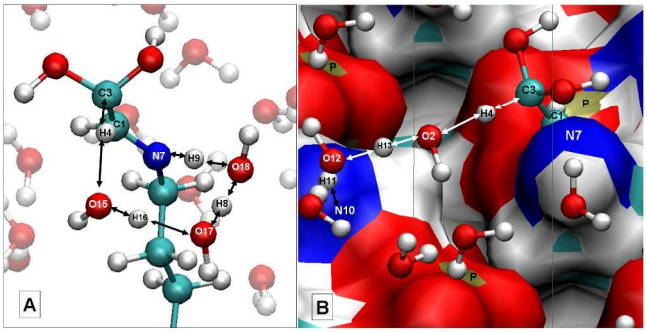

Figure 4. Transition states of the formation of an enamine-diol intermediate. A. From reaction between glyoxal and L-lysine (TS8L). Reactive atoms are labelled, and arrows represent proton transfers. B. From reaction between glyoxal and phosphatidylethanolamine surface (TS10P).

c) Rearrangement to carboxymethyl products. The last step yields to the formation of carboxymethyl compounds, CML in the case of L-lysine/glyoxal system and CM-PE in the case of PE-surface/glyoxal system. The starting points of this intramolecular rearrangement for both cases were Schiff bases, in a neutral form in the case of L-lysine/glyoxal system, and in a protonate form in the case of PE surface/glyoxal system (structures S7L and S9P in schemes 2 and 3, respectively). They can further react and rearrange to an intermediate enamine-diol, followed by their enol-keto tautomerization to carboxymethyl products, CML (S11'L in scheme 2) and CM-PE (S13'P in scheme 3) respectively. The mechanism of this reaction step is similar to the mechanism proposed for the Amadori rearrangement from N-glycosylamine, which undergoes enolization and ketonization to isomeric Amadori compound (l-amino-l-deoxyglycosulose). As in the previous steps, proton transfers are done through a hydrogen bond network. In the case of CML, this transfer is only intramolecular (Fig. 4A). In the case of CM-PE, the generation of the enamine-diol intermediate requires a proton transfer, having as acceptor the neutral amine group from an

adjacent PE molecule (Fig. 4B). It also makes possible to regenerate the catalytic acidic charged amine group of this PE molecule, formed on PE-surface in the previous step.

Table 2. Geometric parameters of the structures presented in scheme 2 for the reaction of formation of N(ε)-carboxymethyl-Lysine from glyoxal and L-lysine (distances in Å and angles in º).

Parameter	S1L	TS2L	S3L	TS4L	S5L	TS6L	S7L	TS8L	S9L	S9´L	TS10'L	S11'L
C1-O2	1.23	1.28	1.35	1.41	1.45	1.89	3.82	5.06	4.21	4.93	2.64	4.09
C1-H6	1.11	1.11	1.11	1.10	1.10	1.10	1.10	1.10	1.09	1.09	1.10	1.10
C1-C3	1.52	1.54	1.56	1.55	1.55	1.52	1.51	1.51	1.35	1.35	1.39	1.53
C3-O5	1.40	1.42	1.42	1.42	1.42	1.41	1.41	1.39	1.36	1.37	1.31	1.23
C1-N7	3.19	1.94	1.56	1.49	1.45	1.35	1.27	1.28	1.43	1.43	1.46	1.48
N7-H8	1.03	1.04	1.05	1.36	1.93	3.00	4.73	3.08	3.95	3.08	3.48	3.63
N7-H9	1.03	1.04	1.05	1.03	1.03	1.10	1.78	1.16	1.03	1.05	1.03	1.03
O2-H10	1.87	1.67	1.61	1.10	1.02	0.99	0.99	0.98	1.00	0.97	1.02	1.01
H10-O11	0.99	1.01	1.02	1.43	1.63	1.84	1.78	8.63	1.72	8.83	3.06	3.06
O11-H12	1.79	1.76	1.77	1.11	1.01	1.01	1.00	1.00	0.99	0.99	1.01	1.00
H12-O13	1.00	1.00	1.00	1.42	1.68	1.70	1.71	1.80	1.84	1.80	1.70	1.72
O13-H14	1.70	1.71	1.70	1.06	1.00	1.00	1.00	0.98	0.99	0.97	1.00	1.00
H14-O15	1.01	1.01	1.01	1.44	1.76	1.75	1.76	3.32	1.81	3.34	1.78	1.79
O15-H16	1.68	1.76	1.75	1.07	1.00	1.00	1.00	1.02	3.07	1.61	3.09	3.08
H16-O17	1.01	1.00	1.00	1.43	1.74	1.75	1.74	1.62	1.02	1.02	1.04	1.04
O17-H8	2.14	2.00	1.89	1.15	1.00	0.98	0.97	1.11	1.77	1.61	5.59	5.66
H9-O18	3.03	2.04	1.84	2.15	2.23	1.46	1.01	1.37	3.82	1.68	3.11	3.30
O18-H19	0.99	1.00	1.00	0.99	0.99	1.01	1.75	1.61	3.35	1.68	3.43	4.25
H19-O20	1.91	1.82	1.79	1.87	1.85	1.70	1.00	1.02	1.00	1.00	1.12	1.80
O20-H21	0.98	1.00	1.01	0.99	0.99	1.03	1.88	1.71	2.86	1.73	2.69	3.32
H21-O2	1.94	1.72	1.69	1.84	1.87	1.56	0.99	1.01	0.98	1.00	1.09	3.08
C3-H4	1.10	1.10	1.10	1.10	1.10	1.10	1.11	1.29	4.63	2.18	3.40	4.99
H4-O15	5.46	5.08	5.02	4.91	5.17	5.33	5.43	1.96	0.99	0.99	1.04	1.00
O18-H8	3.74	3.72	3.50	4.19	4.78	5.14	7.18	1.32	1.02	1.02	1.01	1.00
O20-H22	4.61	4.48	4.60	4.69	4.75	4.73	5.51	5.45	1.54	4.98	1.19	0.99
H22-O5	0.98	0.98	0.98	0.98	0.98	0.98	0.98	1.01	1.03	1.03	1.23	1.81
H21-C1	2.95	2.69	2.67	2.88	2.91	2.79	3.93	4.92	2.31	4.00	1,563	1.10
H19-O2	3.29	3.30	3.22	3.29	3.34	3.16	3.25	3.16	1.91	3.57	1.40	0.99
N7-C1-O2	105.0	111.4	112.7	115.4	115.7	111.2	72.4	44.4	99.0	67.7	102.9	93.3
N7-C1-C3	93.7	100.0	105.5	108.1	109.4	117.6	123.7	121.5	125.5	126.8	121.1	112.8
H6-C1-O2	120.6	117.6	113.0	108.5	106.9	94.7	95.2	72.6	95.0	135.6	104.4	125.1

The enamine-diol formation from the Schiff base through the transition state TS8L in the case of L-lysine/glyoxal system (scheme 2) is an example of an imine-enamine tautomerism. According to other theoretical works[85-87], the rate of converting the imine to enamine depends on how easy it is for an α carbon in the imine to deprotonate, and that is influenced directly by its substituents, which could contribute to lower the basicity of the α carbon during the reaction. In the studied molecular systems, this α carbon corresponds to C3 atoms (structures S7L and S9P in schemes 2 and 3, respectively). In both systems, these atoms have two electronegative hydroxyl groups, which could render inductively electron-withdrawing during the deprotonation of the adjacent carbon atom, dispersing theirs negative charges, and facilitating the proton release (TS8L and TS10P in schemes 2 and 3, respectively). During this imine-enamine tautomerism, the hydroxyl groups, adjacents to C3 atoms, have a conversion from weak electron-withdrawing when it is attached to an sp^3 carbon (S7L and S9P structures in schemes 2 and 3, respectively) to electron releasing group due to the resonance effect when it is attached to an sp^2 carbon (S9L and S11P structures in schemes 2 and 3, respectively).

The relative free energy barriers for the enamine-diol formation (from S7L to S9L and from S9P to S11P) had values of 14.11 and 10.07 kcal mol^{-1} (Fig. 2, table 1). This lower free energy barrier could be explained considering that the starting structure is a Schiff base intermediate which has an iminium group with a protonated nitrogen, more reactive than the neutral imine group of the Schiff base from L-Lysine. These values are similar to those we obtained for the formation of a 1,2-enaminol intermediate as a part of the generation of Amadori

products from D-erythrose and glycine and PE reaction (12.82 and 17.50 kcal mol^{-1}, respectively)[34]. However, these values are low in comparison to results obtained for the reaction between ribose and glycine, where the energy barrier for a similar part of the reaction had a value of 58.3 kcal mol^{-1} at the B3LYP/6-31+G(d) level of theory[88].

Table 3. Geometric parameters of the structures presented in scheme 3 for the reaction of carboxymethyl-PE formation from glyoxal and PE (distances in Å and angles in º).

Parameter	S1P	TS2P	S3P	TS4P	S5P	TS6P	S7P	TS8P	S9P	TS10P	S11P	S11'P	TS12'P	S13'P
C1-O2	1.22	1.28	1.35	1.38	1.40	1.43	1.43	2.12	2.24	3.28	3.87	5.26	5.36	5.41
C1-H6	1.11	1.10	1.11	1.10	1.10	1.10	1.10	1.09	1.09	1.05	1.09	1.09	1.09	1.10
C1-C3	1.53	1.53	1.55	1.55	1.55	1.54	1.54	1.52	1.52	1.49	1.35	1.36	1.39	1.51
C3-O5	1.43	1.40	1.44	1.43	1.44	1.44	1.44	1.44	1.40	1.43	1.39	1.36	1.30	1.23
C1-N7	4.00	2.11	1.56	1.53	1.51	1.46	1.45	1.31	1.29	1.30	1.41	1.44	1.47	1.47
N7-H8	1.03	1.03	1.04	1.05	1.06	1.03	1.03	1.03	1.05	1.04	1.02	1.02	1.03	1.03
N7-H9	1.02	1.04	1.07	1.09	1.08	1.57	1.65	2.86	3.37	3.66	4.70	5.15	5.45	5.78
N10-H11	1.05	1.05	1.06	1.09	1.60	1.40	1.07	1.12	1.68	1.34	1.05	1.05	1.05	1.04
H11-O12	1.84	1.88	1.78	1.61	1.06	1.15	1.66	1.60	1.04	1.18	1.89	1.86	1.87	1.86
O12-H13	0.99	1.00	1.04	0.98	0.99	0.99	1.00	1.25	1.99	1.34	1.00	0.99	0.99	1.03
H13-O2	5.56	1.76	1.55	1.98	1.83	1.76	1.72	1.17	0.98	1.21	1.71	1.87	1.90	1.86
O12-H14	1.01	1.00	1.00	1.23	1.70	1.77	1.80	1.67	4.80	5.51	5.10	3.21	3.30	3.23
H14-O15	1.64	1.77	1.79	1.22	1.01	1.00	1.00	1.01	0.98	0.98	0.98	1.01	1.02	1.01
O15-H16	1.01	1.00	1.00	1.41	1.64	1.69	1.70	1.77	4.72	4.48	3.36	6.23	6.34	6.35
H16-O17	1.65	1.75	1.76	1.10	1.01	1.01	1.01	1.00	1.00	0.99	0.99	0.99	1.00	1.00
O17-H18	1.01	1.00	1.03	1.46	1.68	1.74	1.76	1.77	3.52	3.82	1.74	3.07	3.21	3.25
H18-O2	4.33	1.75	1.57	1.11	1.01	1.00	1.00	1.00	0.99	0.99	1.00	0.98	0.97	0.98
H9-O19	2.03	1.79	1.64	1.58	1.60	1.05	1.02	0.98	0.99	0.99	0.98	0.99	1.08	3.03
O19-H20	0.99	1.00	1.00	1.01	1.00	1.22	1.64	1.81	1.76	1.71	1.81	1.77	1.40	0.99
H20-O21	1.87	1.79	1.74	1.70	1.73	1.22	1.01	0.99	1.01	1.00	0.99	0.99	1.12	1.76
O21-H22	0.99	0.99	1.00	1.01	1.00	1.13	1.70	1.92	1.71	2.31	1.72	6.31	6.37	6.32
H22-O12	1.86	1.81	1.76	1.71	1.79	1.38	1.01	0.99	0.99	0.98	0.99	1.02	1.01	1.03
H9-C1	4.64	2.64	2.17	2.14	2.11	2.48	2.52	2.92	5.85	4.73	3.31	2.10	1.56	1.11
O21-H23	7.31	5.48	5.40	5.31	5.37	5.23	5.05	4.54	7.97	7.25	5.63	1.62	1.15	0.98
H23-O5	0.98	0.98	0.98	0.97	0.98	0.98	0.98	0.98	1.01	0.98	0.98	1.02	1.29	2.05
O2-H4	6.27	7.06	7.05	7.15	6.96	7.01	6.97	6.31	2.93	1.73	0.99	0.98	0.98	0.98
H4-C3	1.10	1.10	1.10	1.10	1.10	1.10	1.10	1.10	1.10	1.27	3.84	5.65	5.84	6.14
N7-C1-O2	133.5	106.4	110.9	111.0	110.5	113.8	114.3	110.2	112.9	98.5	86.1	106.8	98.2	95.5
N7-C1-C3	94.1	100.5	106.1	107.9	109.6	110.6	110.6	122.6	123.7	123.7	124.3	124.2	121.1	113.2
H6-C1-O2	121.9	118.5	113.3	108.6	108.1	105.6	105.2	88.7	71.2	71.2	133.9	102.3	108.0	141.4

In this step of the mechanism, a change in the position of the water molecules involved in the proton transfer (O5 to C1) is required. In Table 1, Figure 2 and scheme 2 and 3, we showed the energetic and structural parameters of the S9L and S11P intermediates. In the CML formation the energy difference between S9L and S9'L intermediates is 2.07 kcal mol^{-1}. Scheme 2 shows as two waters near the C1 must be reoriented for the purpose of facilitating the proton transfer shown in TS10'L. In a similar way this restructuring of two waters above the PE-surface also occurs, being the energetic difference between the intermediates S11P and S11'P of 3.08 kcal mol^{-1} (Scheme 3).

During the conversion of the Schiff base to enamine-diol, the O5 of the hydroxyl group increases the partial negative charge and therefore the acidity of this group. This conversion also leads to C3, covalently bonded to O5 atom, to increase its partial charge. The generated polarization between C3 and O5 atoms results in a coulombic attraction and a decrease of the bond length. The bond lengths have slightly changed from 1.41 and 1.40 Å in the Schiff bases structures of both systems (S7L and S9P, respectively) to values of 1.36 Å in both enamine-diol intermediates (S9'L and S11'P, respectively). Thus, the hydroxyl groups (O5-H22 in L-lysine/glyoxal system and O5-H23 in PE-surface/glyoxal system) of the generated enamine-diol intermediates have increased their acidities respect to the

same groups in the previous Schiff bases. They are able to participate as proton donors and an electron releasing groups in order to yield the carbonyl groups of carboxylic compounds CML and CM-PE (S11'L and S13'P in schemes 2 and 3, respectively).

As other enamines, the enamine-diol intermediates generated from the Schiff bases of L-lysine/glyoxal and PE/glyoxal systems are expected to be also in equilibrium with their keto tautomers through an enol-keto tautomerism (S9'L to S11'L and S11'P to S13'P in schemes 2 and 3, respectively). The tautomerization proceeds via a proton transfer from O5 to C1 atoms, having two water molecules as a bridge in the hydrogen bond network (transition states TS10'L and TS12'P in Fig 2 and 3, respectively). This tautomerism in both cases yield to carboxymethylated compounds, CML and CM-PE, with relatively low free energy barriers (7.47 and 5.24 kcal mol^{-1}, respectively (Fig 2, table 1)). The evolution of this tautomerism could be appreciated through changes of the distance between atoms involved in it. (See S9'L, TS10'L, S11'L in table 2 and S11'P, TS12'P and S13'P in table 3). Taking an insight of these data for structures S9'L and S11'P, it is evidenced they have several reassembly structural features (bond lengths: C1-C3, C3-O5, O5-H22/O5-H23) with TS10'L and TS12'P respectively. The carboxymethyl final products in both systems (S11'L and S13'P) are 22.22 and 31.05 kcal mol^{-1} more stable than the reactives.

The assistance of explicit water molecules for the enol-keto tautomerism has been shown in pyruvate, acetone, acetylacetone, and vinyl alcohol[89-91]. A work of our group about the Amadori rearrangement in PE-surface/D-erythrose and glycine/D-erythrose also evidenced the influence of the PE surface on the free energy barrier, 4.29 kcal mol^{-1} lower than in the pure water glycine/D-erythrose system[34]. In the case of generation of CML and CM-PE, this difference is even lower, 2.22 kcal mol^{-1} (Fig 2 and table 1).

As in other molecular systems[38,73,83,92], carbino-diol amine dehydration in L-lysine/glyoxal and PE/glyoxal systems is the rate-determining step, giving to the whole process an activation energy of 22.42 and 17.12 kcal mol^{-1}, respectively.

In order to study the lipid bilayer's structural complexity, Marrink and Berendsen proposed to divide the membrane into four different regions[78]. The developed model of PE surface by our group belongs to the second region. This region is an interface which begins where water density is equal to that of headgroups and reaches the carbonyl groups. The interface also includes bounded ions and organized water molecules. This apparent simple interface is actually a region with complex structure, sensible to changes in its physicochemical properties as a result of changes in its composition. For example, when water concentration decreases, dielectric permitivity changes from nearly 80 to about 2 (over a distance of about 1 nm)[93], and dipole potential affects electrostatic potential at the immediate vicinity of the membrane or within the interface[45].

According to our results, the role of water in the two studied reactions for carboxymethyl compounds formation is not only as solvent. The water has a catalytic role during all described proton transfers, acting as bridge between proton donor and acceptor groups, and stabilizing electrostatically the transition states and intermediates structures through hydrogen bonds. In the case of PE-surface, these interactions are extended to the polar and charged headgroups of PE. There are two consequences of this fact. Firstly, the organization and mobility of water molecules above PE-surface is different to pure water, the amount of water, its structure and mobility change with its distance from the aqueous phase[45]. Phospholipids bind approx. 0.5-3 water molecules/lipid very tightly, the energy to remove these water molecules is on average 40 kJ mol^{-1} [94,95], which is equivalent to the energy of a hydrogen bond. Secondly, the hydrogen bond network above PE-surface enables ethanolamine group of PE head to lay flat on the membrane surface, reducing the entropic effect associated with its possible freely rotation in absence of these interactions, that appears in choline moiety of phosphatidylcholine due the lack of hydrogen bonds[96]. Intermolecular interactions within the interface should, therefore, be treated as a combination of electrostatic forces and hydration, along with static and dynamic steric constrains[45,95,96].

It is known that introducing of surface as a cofactor to biochemical reactions brings changes in their characteristics[45]. Membrane-associated reactions are controlled by the transmembrane and lateral distribution of reactive molecules, which depends ultimately on the state of the lipid bilayer and the efficiency of its transport mechanisms. On the other hand, biochemical reactions occurring in aqueous solution are controlled in almost exclusively by diffusion[45,97]. In this work, we consider the possible catalytic effect of the surface, reducing the free energy barriers in the reaction pathway. This effect is done through the phospholipids polar and charged headgroups and the water molecules of the surface surroundings. It has been evidenced theoretically, comparing the free energy profiles of Schiff base formation, Amadori rearrangement and hydrogen peroxide decomposition above PE surface and pure water models[34,37,79].

Summarizing, the catalytic effect of PE surface in the reaction of formation of CM-PE is accomplished in three ways: (i) accumulation of water molecules on the surface, increasing their organization, reducing their mobility and polarizing their bonds as a result of an interaction with the PE charged groups; (ii) direct acid catalysis through amine groups of PE molecules adjacent to reactive PE molecule acting as donors or acceptors in the proton transfers, and water molecules in the surface surroundings acting as bridges in the proton exchange between donor and acceptor protons in the reaction; (iii) passive catalytic effect through a charge stabilization of different intermediate structures of reaction, due to direct electrostatic interactions with the charged groups generated in the different steps of the reaction.

Conclusions

We have studied the mechanism for the reaction of formation of carboxymethyl compounds, CML and CM-PE, from reactions between mono hydrated form of glyoxal and L-lysine and PE.

Both mechanisms take place in three steps: i) Carbino-diol-amine formation ii) dehydration of the adduct, iii) Rearrangement into carboxymethyl final products. The rate-limiting step for the formation of CML and CM-PE was the dehydration step, having an activation energy of 22.42 kcal mol^{-1}, and 17.12 kcal mol^{-1}, respectively. The comparison of both reactions in their equivalent steps shows a catalytic role of the PE surface, highlighted in the case of the dehydration step where its relative free energy barrier had a value of 5.30 kcal mol^{-1} lower than the obtained in L-lysine/glyoxal system. This catalytic effect is done through PE surface components as amine and phosphate groups, which might enhance the reaction, facilitating the water molecules accumulation in their proximity, participating through amine groups as donors or acceptors in proton transfers, and stabilizing charge in intermediates and transition states of the different reaction steps. Taking into account this effect, we conclude that reactions above the phopholipid surfaces could have an active role and it should not be considered to be a nonspecific charged phase boundary. Our results also give support to consider the pathway of formation of CML and CM-PE from reactions between glyoxal and L-lysine and PE respectively, as an alternative pathway for generation of these AGEs.

Acknowledgements

The financial support of Govern de les Illes Balears (AAEE27/2014) is gratefully acknowledged. C.S.-C. is grateful to the Spanish Ministry of Foreign Affairs and Cooperation for the award of a MAE-AECI fellowship. We are grateful to Centro de cálculo de Computación de Galicia (CESGA) and the Centro de cálculo de Computación de Cataluña (CESCA) for allowing the use of their computational facilities.

Notes and references

[a] Institut d'Investigació en Ciències de la Salut (IUNICS). Departament de Química. Universitat de les Illes Balears. E-07122 Palma de Mallorca, Spain. E mail: joaquin.castro@uib.es

[b] Instituto Andaluz de Ciencias de la Tierra (CSIC-UGR), Avda. de las Palmeras 4, Armilla, 18100 Granada, Spain

1 Z. Wang, Y. Jiang, N. Liu, L. Ren, Y. Zhu, Y. An and D. Chen, *Atherosclerosis*, 2012, **221** (2), 387.

2 V. M. Monnier, *Arch. Biochem. Biophys*., 2003, **419**, 1.

3 A. E. Ferreira, A. M. Ponces Freire and E. O. Voit, *Biochem. J.,* 2003, **376**, 109.

4 N. M. Hanssen, L. Engelen, I. Ferreira, J. L. Scheijen, M. S. Huijberts, M. M. van Greevenbroek, C. J. van der Kallen, J. M. Dekker, G. Nijpels, C. D. Stehouwer and C. G. Schalkwijk, *J. Clin. Endocrinol. Metab.,* 2013, **98** (8), E1369.

5 I. Roncero-Ramos, C. Delgado-Andrade, F. J. Tessier, C. Niquet-Léridon, C. Strauch, V. M. Monnier, and M. P. Navarro, *Food Funct.,* 2013, **4** (7), 1032.

6 R. Nagai, K. Ikeda, T. Higashi, H. Sano, Y. Jinnouchi, T. Araki and S. Horiuchi, Biochem. *Biophys. Res. Commun.,* 1997, **234** (1), 167.

7 M. U. Ahmed, S. R. Thorpe and J. W. Baynes, *J. Biol. Chem.,* 1986, **261** (11), 4889.

8 Y. Al-Abed and R. Bucala, *Bioorg. Med. Chem. Lett*., 1995, **5** (18), 2161.

9 K. J. Wells-Knecht, D. V. Zyzak, J. E. Litchfield, S. R. Thorpe and J. W. Baynes, *Biochem.,* 1995, **34** (11), 3702.

10 S. P. Wolff and R. T. Dean, *Biochem. J.*, 1987, **245** (1), 243.

11 M. Namiki and T. Hayashi, *ACS Symp. Ser.,* 1983, **215**, 21.

12 M. A. Glomb and V. M. Monnier, *J. Biol. Chem.,* 1995, **270**, 10017.

13 N. Shoji, K. Nakagawa, A. Asai, I. Fujita, A. Hashiura, Y. Nakajima, S. Oikawa and T. Miyazawa, *J. Lipid. Res.,* 2010, **51**, 2445.

14 R. Pamplona, J. R. Requena, M. Portero-Otín, J. Prat, S. R. Thorpe and M. J. Bellmunt, *Eur. J. Biochem.,* 1998, **255**, 685.

15 J. R. Requena, M. U. Ahmed, C. W. Fountain, T. P. Degenhardt, S. Reddy, C. Perez, T. J. Lyons, A. J. Jenkins, J. W. Baynes, and S. R. Thorpe, *J. Biol. Chem.* 1997, **272**, 17473.

16 R. Nagai, K. Ikeda, Y. Kawasaki, H. Sano, M. Yoshida, T. Araki, S. Ueda and S. Horiuchi, *FEBS Lett.* 1998, **425** (2), 355.

17 P. J. Thornalley, *Drug. Metabol. Drug. Interact.* 2008, **23** (1-2), 125-150.

18 C. M. Utzmann and M. O. Lederer, *J. Agric. Food Chem.* 2000, **48** (4), 1000.

19 M. O. Lederer and M. Baumann, *Bioorg. Med. Chem.* 2000, **8** (1), 115.

20 V. Levi, A. M. Villamil Giraldo, P. R. Castello, J. P. Rossi and F. L. González Flecha, *Biochem. J.* 2008, **416** (1), 145.

21 Y. Wang and C. T. Ho, *Chem. Soc. Rev.* 2012, **41** (11), 4140.

22 Z. Turk, *Physiol. Res.* 2010, **59** (2), 147.

23 M. X. Fu, J. R. Requena, A. J. Jenkins, T. J. Lyons, J. W. Baynes and S. R. Thorpe, *J. Biol. Chem.* 1996, **271**, 9982.

24 M. M. Anderson, S. L. Hazen, F. F. Hsu and J. W. Heinecke, *J. Clin. Invest.* 1997, **99** (3), 424.

25 S. R. Thorpe, T. J. Lyons and J. W. Baynes, *Glycation and glycoxidation in diabetic vascular disease. In: Oxidative Stress and Vascular Disease;* KEANEY JF, (ed) Kluwer Academic Publishers, Norwell, MA., 2000, 259.

26 A. Napolitano, P. Manini and M. d'Ischia *Curr. Med. Chem.* 2011, **18** (12), 1832.

27 P. J. Thornalley, *Novartis Found. Symp.* 2007, **285**, 229.

28 T. Miyazawa, K. Nakagawa, S. Shimasaki and R. Nagai, *Amino Acids*. 2012, **42**, 1163.

29 S. Mizumoto and K. Sugahara, *FEBS J.* 2013, **280** (10), 2462.

30 A. Prasad, P. Bekker and S. Tsimikas, *Cardiol. Rev.* 2012, **20**, 177.

31 P. Sookwong, K. Nakagawa, I. Fujita, N. Shoji and T. Miyazawa, *Lipids.* 2011, **46** (10), 943.

32 S. Lertsiri, M. Shiraishi and T. Miyazawa, *Biosci. Biotechnol. Biochem.* 1998, **62**, 893.

33 A. Ravandi, A. Kuksis, L. Marai, J. J. Myher, G. Steiner, G. Lewisa and H. *FEBS Lett.* 1996, **381**, 77.

34 C. Solís-Calero, J. Ortega-Castro, A. Hernández-Laguna and F. Muñoz, F., *J. Phys. Chem. C* 2013, **117** (16), 8299.

35 B. Vilanova, J. M. Gallardo, C. Caldés, M. Adrover, J. Ortega-Castro, F. Muñoz, J. Donoso, *J. Phys. Chem. A* 2012, **116**, 1897.

36 C. Caldés, B. Vilanova, M. Adrover, F. Muñoz and J. Donoso, *Bioorg. Med. Chem.* 2011, **19**, 4536.

37 C. Solís-Calero, J. Ortega-Castro and F. Muñoz, *J. Phys. Chem. B* 2010, **114**, 15879.
38 A. Salvà, J. Donoso, J. Frau and F. Muñoz, *J. Phys. Chem. A* 2003, **107**, 9409.
39 A. Salvà, J. Donoso, J. Frau and F. Muñoz, *J. Phys. Chem. A* 2004, **108**, 11709.
40 M. A. Vázquez, J. Donoso, F. Muñoz, F. García Blanco, M. A. Garcia del Vado and G. Echevarría, *J. Chem. Soc., Perkin. Trans. 2* 1991, 1143.
41 M. A. Vázquez, F. Muñoz, J. Donoso and F. García Blanco, *J. Chem. Soc., Perkin Trans. 2* 1991, 275.
42 M. A. Vázquez, F. Muñoz, J. Donoso and F. García Blanco, *Int. J. Chem. Kinet.* 1990, **22**, 905.
43 M. A. Vázquez, F. Muñoz, J. Donoso, F. García Blanco, M. A. Garcia del Vado and G. Echevarría, *J. Mol. Catal.* 1990, **59**, 137.
44 S. J. Singer and G. L. Nicolson, G. L. *Science*, 1972, **175**, 720.
45 M. Langner and K. Kubica, *Chem. Phys. Lipids.* 1999, **101** (1), 3.
46 M. Subramanian, A. Jutila and P. K. Kinnunen, *Biochem.* 1998, **37**, 1394.
47 A. Toker and L. C. Cantley, *Nature* 1997, **387**, 673.
48 A. Y. Mulkidjanian, J. Heberle and D. A. Cherepanov, *Biochim. Biophys. Acta* 2006, **1757**, 913.
49 G. L. Squadrito, E. M. Postlethwait and S. Matalon, *Am. J. Physiol. Lung. Cell. Mol. Physiol.* 2010, **299** (3), L289.
50 R. Zamora and F. J. Hidalgo, *Chem. Res. Toxicol.* 2003, **16**, 1632.
51 E. Wachtel, D. Bach, R. F. Epand, A. Tishbee and R. M. Epand, *Biochem.* 2006, **45**, 1345.
52 M. Yoshimoto, Y. Miyazaki, A. Umemoto, P. Walde, R. Kuboi, and K. Nakao, *Langmuir* 2007, **23** (18), 9416.
53 M. Yoshimoto, Y. Miyazaki, M. Sato, K. Fukunaga, R. Kuboi and K. Nakao, *Bioconjug. Chem.* 2004, **15** (5), 1055.
54 C. Solís-Calero, J. Ortega-Castro and F. Muñoz, *J. Phys. Chem. C* 2011, **115**, 22945.
55 M. Elder, P. Hitchcock, R. Mason, G. G. Shipley, *Proc. R. Soc. Lond. A.* 1977, **354**, 157.
56 B. Delley, *Mol. Simul.* 2006, **32**, 117.
57 A. Klamt and G. Schüürmann, *J. Chem. Soc., Perkin Trans. 2,* 1993, 799.
58 J. Andzelm, C. Kölmel and A. Klamt, *J. Chem. Phys.* 1995, **103**, 9312.
59 B. Delley, *J. Chem. Phys.* 2000, **113**, 7756.
60 B. Delley, *J. Phys. Chem.* 1996, **100**, 6107.
61 B. Delley, *J. Chem. Phys.* 1990, **92**, 508.
62 J. P. Perdew, K. Burke and M. Ernzerhof, *Phys. Rev. Lett.* 1996, **77**, 3865.
63 J. P. Perdew, J. A. Chevary, S. H. Vosko, K. A. Jackson, M. R. Pederson, D. J. Singh and C. Fiolhais, *Phys. Rev. B. Condens. Matter* 1992, **46**, 6671.
64 T. Lin, W. D. Zhang, J. Huang and C. He, *J. Phys. Chem. B.* 2005, **109** (28), 13755.
65 N. Matsuzawa, J. Seto and D. A. Dixon, *J. Phys. Chem. A.* 1997, **101**, 9391.
66 J. Andzelm, N. Govind, G. Fitzgerald and A. Maiti, *Int. J. Quant. Chem.* 2003, **91**, 467.
67 T. A. Halgren and W. N. Lipscomb, *Chem. Phys. Lett.* 1977, **49**, 225.
68 R. Lavery, M. De Oliveira and B. Pullman, *Int. J. Quan. Chem.* 1979, **16**, 459.
69 A. R. Fratzke and P. J. Reilly, *Int. J. Chem. Kinet.* 1986, **18**, 757.
70 H. E. Krizner, D. O. De Haan and J. Kua, *J. Phys. Chem. A.* 2009, **113**, 6994.
71 M. P. Patil and R. B. Sunoj, *J. Org. Chem.* 2007, **72**, 8202.
72 K. N. Rankin, J. W. Gauld and R. J. Boyd, *J. Phys. Chem. A* 2002, **106**, 5155.
73 J. Ortega-Castro, M. Adrover, J. Frau, A. Salvà, J. Donoso and F. Muñoz, *J. Phys. Chem. A.* 2010, **114** (13), 4634.
74 R. Kjellander and S. Marcelja, *Chem. Scr.* 1985, **25**, 73.
75 R. Kjellander and S. Marcelja, *Chem. Phys. Lett.* 1985, **120**, 393.
76 M. C. Wiener and S. H. White, *Biophys. J.* 1991, **59**, 162.
77 M. C. Wiener and S. H. White, *Biophys. J.* 1991, **59**, 174.
78 D. P. Tieleman, S. J. Marrink and H. J. C. Berendsen, *Biochim. Biophys. Acta.* 1997, **1331**, 235.
79 C. Solís-Calero, J. Ortega-Castro, A. Hernández-Laguna and F. Muñoz, *Theor. Chem. Acc.* 2012, **131**, 1263.
80 C. Dohno, A. Okamoto and I. Saito, *J. Am. Chem. Soc.* 2005, **127** (47), 16681.
81 M. A. Vázquez, G. Echevarría, F. Muñoz, J. Donoso and F. García Blanco, *J. Chem. Soc. Perkin Trans 2* 1989, 1617.
82 K. B. Wiberg, *J. Am. Chem. Soc.* 1990, **112**, 3379.
83 R. Z. Liao, W. J. Ding, J. G. Yu, W. H. Fang and R. Z. Liu, *J. Comput. Chem.* 2008, **29**, 1919.
84 M. Shimizu, I. Hachiya and I. Mizota, *Chem. Commun.* 2009, 874.
85 P. Pérez and A. Toro-Labbé, *Theor. Chem. Acc.* 2001, **105**, 422.
86 J. F. Lin, C. C. Wu and M. H. Lien, *J. Phys. Chem.* 1995, **99**, 16903.
87 R. Casasnovas, M. Adrover, J. Ortega-Castro, J. Frau, J. Donoso and F. Muñoz, *J. Phys. Chem. B* 2012, **116**, 10665.
88 X. X. Bao, Z. Q. Chen and H. J. Xie, *Chin. J. Struct. Chem.* 2011, **30**, 827.
89 G. Alagona, C. Ghio and P. I. Nagy, *Phys. Chem. Chem. Phys.* 2010, **12** (35), 10173.
90 C. S. Cucinotta, A. Ruini, A. Catellani and A. Stirling, *Chem. Phys. Chem.* 2006, **7** (6), 1229.
91 O. N. Ventura, A. Lledos, R. Bonaccorsi, J. Bermin and J. Tomasi, *Theor. Chim. Acta* 1987, **72**, 175.
92 M. Y. Gokhale and L. E. Kirsch, *J. Pharm. Sci.* 2009, **98** (12), 4616.
93 H. Brockman, *Chem. Phys. Lipids.* 1994, **73** (1-2), 57.
94 E. A. Disalvo, F. Lairion, F. Martini, E. Tymczyszyn, M. Frías, H. Almaleck and G. J. Gordillo, *Biochim. Biophys. Acta.* 2008, **1778**, 2655.
95 G. L. Jendrasiak, *J. Nutr. Biochem.* 1996, **7**, 599.
96 J. N. Israelachvili and H. Wennerstrom, J. *Phys. Chem.* 1992, **96**, 520.
97 Y. N. Antonenko, P. Pohl and E. Rosenfeld, *Arch. Biochem. Biophys.* 1996, **333**, 225.